ACS APPLIED BIO MATERIALS

www.acsabm.org

Forum Article

A Cell Membrane Fluorogenic Probe for Gram-Positive Bacteria Imaging and Real-Time Tracking of Bacterial Viability

Weiwei Liu,[†] Ruihua Li,[†] Fei Deng, Chunyu Yan, Xuelian Zhou, Lu Miao,* Xiaolian Li,* and Zhaochao Xu*

Cite This: https://dx.doi.org/10.1021/acsabm.0c01269

Read Online

ACCESS | Metrics & More | Article Recommendations | Supporting Information

ABSTRACT: Bacterial infections are a global healthcare problem, resulting in serious clinical morbidities and mortality. Real-time monitoring of live bacteria by fluorescent imaging technology has potential in diagnosis of bacterial infections, elucidating antimicrobial agents' mode of action, assessing drug toxicity, and examining bacterial antimicrobial resistance. In this work, a naphthalimide-derived fluorescent probe **ZTRS-BP** was developed for wash-free Gram-positive bacteria imaging. The probe aggregated in aqueous solutions and exhibited aggregation-caused fluorescence quenching (ACQ). The interaction with Gram-positive bacteria cell walls would selectively disaggregate the probe and the liberated probes were dispersed on the outside of the bacteria cell walls to achieve surface fluorescence imaging. There were no such interactions with Gram-negative bacteria, which indicates that selective binding and imaging of Gram-positive bacteria was achieved. The binding of zinc ions by **ZTRS-BP** can enhance the fluorescent signals on the bacterial surface by inhibiting the process of photoinduced electron transfer. **ZTRS-BP-Zn(II)** complex was an excellent dye to discriminate mixed Gram-positive and Gram-negative bacteria. Also, live and dead bacteria can be differentially imaged by **ZTRS-BP-Zn(II)**. Furthermore, **ZTRS-BP-Zn(II)** was used for real-time monitoring bacteria viability such as *B. cereus* treated with antibiotic vancomycin.

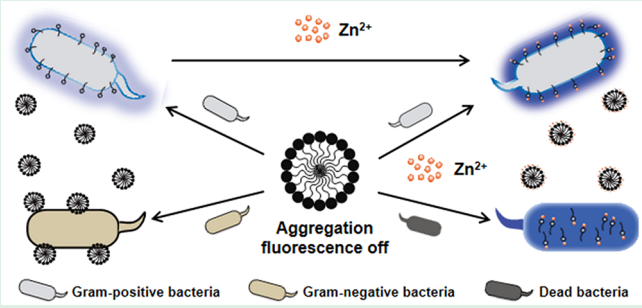

KEYWORDS: *fluorogenic probe, Gram-positive bacteria, fluorescent imaging, real-time tracking, bacterial viability*

1. INTRODUCTION

The increase in pathogen infections in clinical practice has become a public health issue that has caused global concern.[1] Pathogenic bacteria are the main cause of human disease and death. For example, *Staphylococcus aureus*, *Bacillus cereus*, and *Mycobacterium tuberculosis* may cause various diseases including infective endocarditis, meningitis, food poisoning, tuberculosis (TB), etc.[2−4] Every year, nearly one million people die from diseases arising from bacterial infections. Moreover, the emergence and wide spread of drug-resistant bacteria (including multidrug-resistant (MDR) bacteria) has promoted the threat of bacterial infection to public health.[5,6] According to the World Health Organization, in 2018, there were about half a million new cases of rifampicin-resistant TB, of which 78% were MDR TB; these accounted for 21.4% of the total TB cases.[7] Quick and accurate infection diagnosis is thus very important for clinical treatment and environmental protection.

Fluorescence probes have emerged as a useful tool for the investigation of pathogenic bacteria because of their high sensitivity, fast response speed, and ability to visually image and dynamically track bacteria.[8−13] A prominent application is to monitor bacterial viability, which is crucial in determining the safety of food and drinking water.[14−16] The usual bacterial detection relies on the identification of genes, marker proteins, or enzymes.[17−19] However, because of the excessive abuse of antibiotics, the problem of bacterial multidrug resistance has become more and more serious.[20,21] Bacterial detection that relies on markers often cannot reflect the changes of bacteria after adapting to drug resistance. The pathogenicity of bacteria is usually related to the composition of the cell walls, which are heterogeneous in composition and dynamic changes, including the types and ratios of membrane phospholipids and membrane proteins, and the charges on the surface of different bacteria.[22,23] Thus, the cell walls play a role in the fingerprint of the bacteria, and the bacteria can be discriminated by identifying the cell walls of the bacteria.

Fluorescence imaging techniques have facilitated fluorescent probes to monitor the subcellular localization and dynamics of bacteria cell walls.[24−31] For example, the surfaces of anaerobe

Special Issue: Biospecies Sensors

Received: September 30, 2020
Accepted: October 29, 2020

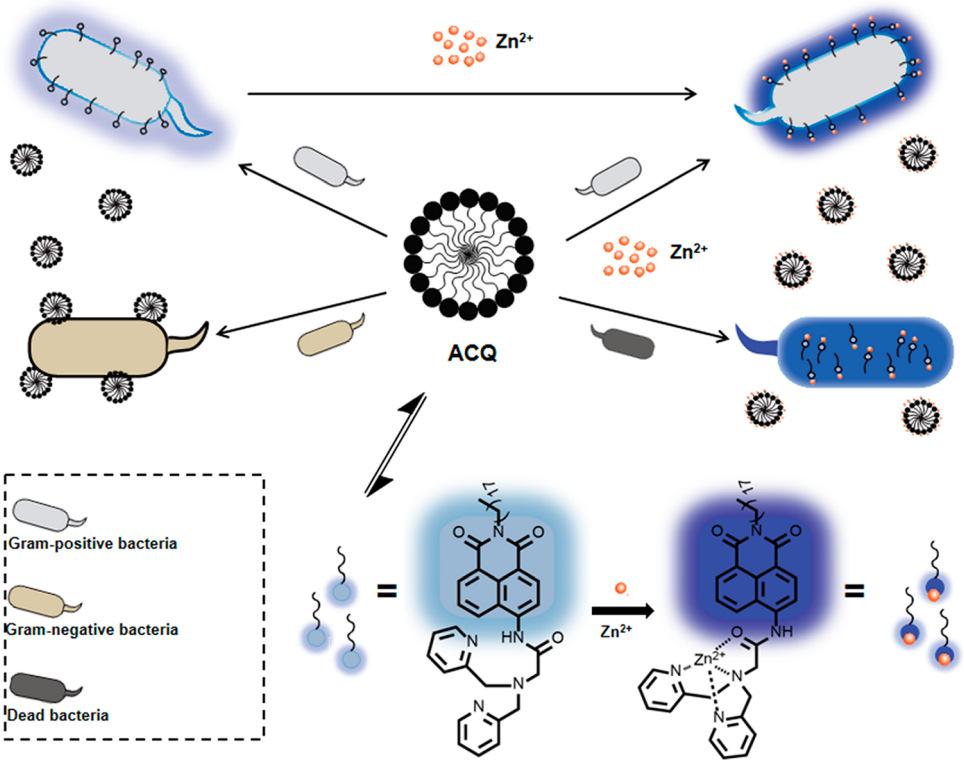

Figure 1. Schematic illustration of wash-free and selective imaging of Gram-positive bacteria by the fluorogenic probe **ZTRS-BP**.

Bacteroides fragilis were modified with azide-containing sugars and then fluorescently labeled by a cyclooctyne-containing fluorophore via bio-orthogonal click chemistry.[32] These location-unspecific or unbound probes can produce background interference. To address this issue, fluorogenic probes based on azido Si-rhodamine have been developed via biocompatible copper-free click chemistry for the no-wash visualization of bacterial peptidoglycan (PG), which are initially fluorescence-silent but activated upon target recognition with specific fluorescence responses.[33] However, these probes cannot be used in intact bacterial cells, because they depended on bioorthogonal click chemistry to locate small molecular probes in bacterial surfaces. We recently reported an imidazolium-derived pyrene compound as a fluorogenic probe for bacteria cell wall imaging.[34] Unfortunately, the UV excitation of this probe limited its application.

In this paper, we reported a Gram-positive bacteria selective probe **ZTRS-BP** for bacteria cell wall fluorogenic imaging using the aggregation-disaggregation strategy to achieve the membrane-specific fluorogenicity. In our previous work, we reported the naphthalimide-derived compound **ZTRS** acted as an environment-selective probe.[35−37] Here, a hydrophobic alkyl chain as the membrane-anchored domain was introduced to get the probe **ZTRS-BP**. As shown in Figure 1, probe **ZTRS-BP** aggregated in aqueous solutions and exhibited aggregation-caused fluorescence quenching (ACQ). The interaction with Gram-positive bacteria cell walls would selectively disaggregate the probe and the liberated probes were dispersed on the outside of the bacteria cell walls to achieve surface fluorescence imaging. There were no such interactions with Gram-negative bacteria, which achieved selective binding and imaging of Gram-positive bacteria. The binding of zinc ions can enhance the fluorescent signals on the bacterial surface by inhibiting the process of photoinduced electron transfer. Aggregates that do not bind to the bacteria cell walls still exhibit aggregation-induced quenched fluorescence even after complex with zinc ions to achieve the fluorogenicity. It was worth noting that this aggregation-disaggregation strategy allowed the probe to label only on the surface of live bacteria, but can enter the content of dead bacteria, thereby achieving selective identification and imaging of live and dead bacteria. These properties make the probe a useful tool for real-time tracking of bacterial viability.

2. EXPERIMENTAL SECTION

2.1. Materials and Methods. Unless otherwise stated, all reagents were purchased from commercial suppliers and used without further purification. ^{1}H NMR and ^{13}C NMR spectra were recorded on Bruker 400 spectrometer, where the chemical shift is based on tetramethyl silicon. The fluorescence spectrum is from Agilent CARY Eclipse spectrophotometer; the ultraviolet absorption spectrum is from Agilent CARY 60 UV−vis. The nano laser particle size analyzer is Malvern. The fluorescence confocal microscope is Olympus FV1000, 100 times oil lens (NA = 1.40).

Bacillus cereus (*B. cereus*, 1.1626) was purchased from China General Microbiological Culture Collection Center (CGMCC). *Staphylococcus aureus* (*S. aureus*, ATCC 25923), *Klebsiella pneumoniae* (*K. pneumoniae*), and *Escherichia coli* (*E. coli* ATCC 25922) were obtained from the Second Hospital of Dalian Medical University

2.2. Optical Detection. **ZTRS-BP** was dissolved in chromatographically pure dimethyl sulfoxide (DMSO) to prepare a 2 mM solution for further detection. The UV−vis absorption and fluorescence spectra of **ZTRS-BP** and **ZTRS-BP**-Zn^{2+} (final concentration of 5 μM) in HEPES buffer solution (20 mM, pH 7.4) were examined. Surfactant SDS was dissolved in water to prepare a 20 mM solution. The fluorescence spectra of **ZTRS-BP** in HEPES buffer solution (20 mM, pH 7.4) with different concentrations of SDS was tested, which was excited by 365 nm light.

2.3. Bacteria Culture. The single spot on the solid LB medium with bacteria was transferred to 5 mL of LB medium and cultured in a

https://dx.doi.org/10.1021/acsabm.0c01269
ACS Appl. Bio Mater. XXXX, XXX, XXX−XXX

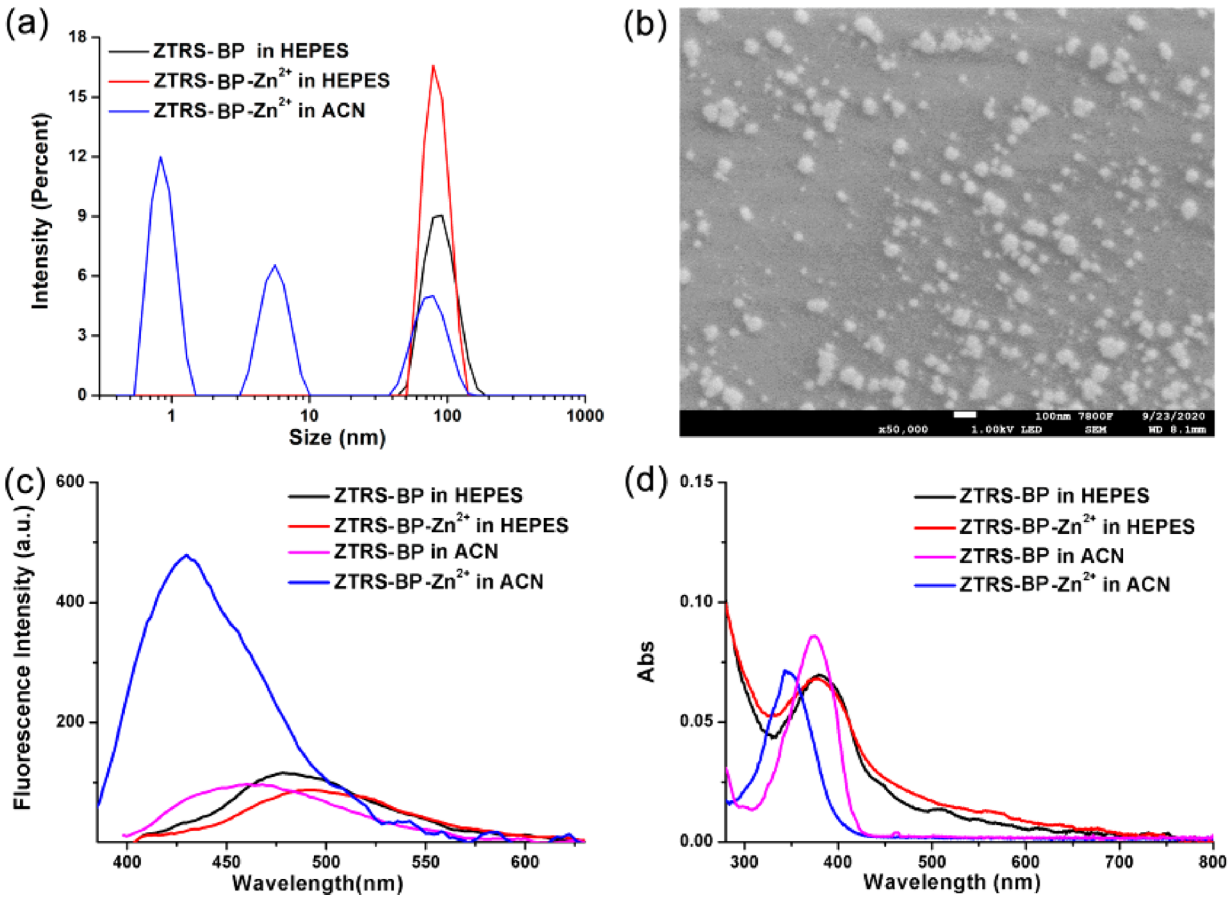

Figure 2. Photophysical properties of **ZTRS-BP**. (a) DLS analysis of **ZTRS−BP** (5 μM). (b) SEM image of **ZTRS−BP** in HEPES. (c) Fluorescence and (d) absorption spectra of **ZTRS-BP** in HEPES and ACN with or without Zn^{2+}.

shaker at 37 °C until the bacteria optical density at 600 nm (OD 600) was 1.0. The bacteria were transferred to a 1.5 mL EP tube and centrifuged at 10000 rpm for 2 min. The bacterial pellets were then suspended in HEPES (20 mM, pH 7.4) and adjusted the OD_{600} value to 0.5. For spectrum detection, the bacteria and probe were mixed in HEPES buffer with or without the addition of $Zn(ClO_4)_2$ at a certain concentration. Before testing, the mixtures were stay at room temperature for 3 min. The fluorescence spectrum were obtained with the excited wavelength of 365 nm.

2.4. Bacteria Imaging. The bacteria culture process was as above description. The bacteria and probe were mixed in HEPES buffer with or without the addition of $Zn(ClO_4)_2$ at a certain concentration, which was incubated at room temperature for 10 min. For the imaging experiment with washing step, the mixture was washed one time and resuspend with HEPES buffer (20 mM, pH 7.4). For the washout experiment, this step is omitted. To take confocal images, we dropped 1.5 μL of the mixed solution on a confocal imaging dish and covered it with a thin layer of agarose gel. The image was collected using a 100× oil lens on an Olympus laser scanning confocal microscope (FV1000) under the conditions of excitation, 405 nm; emission range, 425−525 nm.

2.5. Live and Dead Bacteria Imaging. Imaging of live bacteria *B. cereus* was performed as above. For imaging of dead bacteria of *B. cereus*, the live bacteria were resuspended in 70% isopropanol and shaken with 200 rpm at 28 °C for 1 h to obtain dead bacteria. The dead bacteria were washed twice and then resuspended with HEPES buffer (20 mM, pH 7.4). The mixture of live and dead bacteria was obtained by mixing the live and dead bacteria of *B. cereus* in equal amounts. PI was added to these bacterial liquids and incubated for 10 min under dark conditions. After washing for one time, **ZTRS-BP** and $Zn(ClO_4)_2$ was added to a final concentration of 5 μM, respectively. After incubating for 5 min, 1.5 μL of the mixed solution was dropped on a dish and covered with a thin layer agarose gel, and then observed using confocal microscope under the conditions of excitation, 405 nm; emission range, 425−525 nm; excitation, 543 nm; emission range, 560−650 nm.

2.6. Vancomycin Sterilization and Fluorescence Monitoring. The bacteria culture process was the same as the above description. The bacterial pellets was resuspended in HEPES (20 mM, pH 7.4) and the OD_{600} value was adjusted to 0.5. Vancomycin (Final concentration was 5 μM) was then added to the bacterial solution. The mixture was incubated at room temperature for 1 h. Then **ZTRS-BP** and $Zn(ClO_4)_2$ was added to a final concentration of 5 μM, respectively. After incubating for 10 min, 2 μL of the mixed solution was dropped on a dish and covered with a thin layer agarose gel, and then observed with a confocal microscope under the condition: Excitation: 405 nm, Emission range: 425−525 nm.

3. RESULTS AND DISCUSSION

3.1. Photophysical Properties of ZTRS-BP. The synthesis route of **ZTRS-BP** is shown in Figure S1. The aggregation property of **ZTRS-BP** was investigated by means of dynamic light scattering (DLS) measurements and scanning electron microscopy (SEM) (Figure 2a, b). DLS and SEM analysis showed that **ZTRS-BP** aggregated in HEPES to form nanoparticles with the mean diameter of 80 nm (Figure 2a, b). The addition of Zn^{2+} cannot dissolved the aggregate as shown in Figure 2a, even **ZTRS** binding zinc ion with high affinity, and the size of nanoparticle was still around 80 nm. But when the probe incubated with Zn^{2+} in polar solvent acetonitrile (ACN), there were three peeks found during DLS experiments, 1 nm (12% intensity), 5 nm (6% intensity), and 70 nm

https://dx.doi.org/10.1021/acsabm.0c01269
ACS Appl. Bio Mater. XXXX, XXX, XXX−XXX

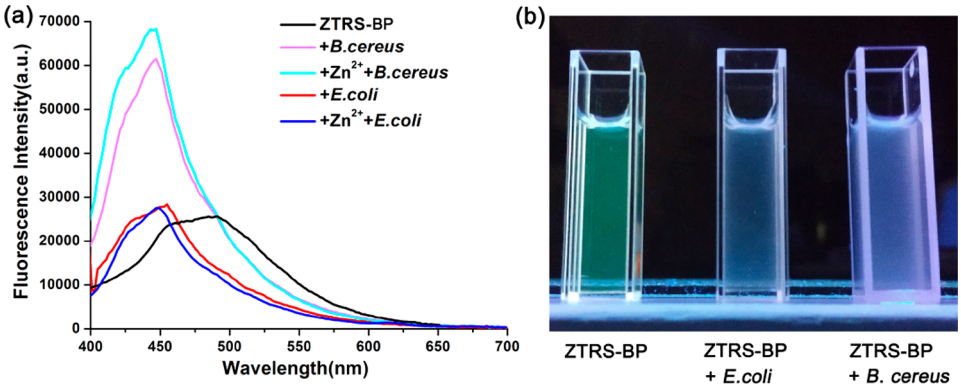

Figure 3. (a) Fluorescence spectra of 5 μM **ZTRS-BP** sensing to Gram-positive bacteria *B. cereus* and Gram-negative bacteria *E. coli*, with or without Zn^{2+} (5 μM) in HEPES (10 mM, pH 7.4) solution. (b) Visible emissions of **ZTRS-BP** with *B. cereus* and *E. coli* in HEPES under UV irradiation.

(4% intensity), respectively. So, with the addition of zinc ions, the size of **ZTRS-BP** nanoparticles changed from 80 to 1 nm, ascribed to the disassembly of **ZTRS-BP** in ACN by zinc binding. We tested the fluorescent spectra of **ZTRS-BP** with the addition of different concentrations of SDS (Figure S2), which was a anionic surfactants to be expected to disassemble the aggregate. We found that the fluorescence of **ZTRS-BP** did not change, even the concentration of SDS increased to 4 mM. These results indicated that the aggregates of **ZTRS-BP** were structurally stable in aqueous solutions, but were easily decomposed when encountered in a fat-soluble environment. This property allowed **ZTRS-BP** to have excellent fluorogenicity when staining bacteria, that is, the hydrophobic interaction with the Gram-positive bacteria made the **ZTRS-BP** aggregates easy to decompose and further stained the surface of the bacteria, while keeping the aggregate structure stable with quenched fluorescence in other environments.

To further test the stability and fluorogenicity of **ZTRS-BP**, we examined its fluorescence and absorption responses to Zn^{2+} in HEPES and ACN. As shown in Figure 2c, due to the stability, the probe displayed aggregation-quenched fluorescence even with the addition of zinc in aqueous solution. In acetonitrile with the addition of zinc ions, the absorption and emission all shifted to short wavelengths with an obvious increase in fluorescence, indicating that the compound bound zinc ions in an amide tautomeric form and disassembled the aggregates.

3.2. Selective Recognition of Bacteria. Bacterial cell walls are composed of phospholipid bilayer and peptidoglycan, but the cell wall structures of Gram-positive and Gram-negative bacteria are indeed completely different. In general, Gram-positive bacteria contain a single cell membrane surrounded by a thick layer of peptidoglycan, whereas Gram-negative bacterial surface contains a thin layer of peptidoglycan sandwiched between two layers of phospholipids. Considering that the bacterial cell wall has some hydrophobic properties, the probe may recognize bacteria by being disaggregated and emitting fluorescence after interacting with the bacteria. The fluorescence spectra of the probe to different bacteria were then recorded. There was an increase in fluorescence of the probe with the addition of Gram-positive bacteria, such as *Bacillus cereus* (*B. cereus*) (Figure 3a). And the addition of the zinc ions further enhanced the fluorescence response signal. The fluorescence spectra of the probe with Gram-negative bacteria such as *Escherichia coli* (*E. coli*) displayed blue-shifted emission, indicating that the weak polar environments near the surface of the Gram-negative bacteria made the fluorescence emission wavelength of **ZTRS-BP** blue shift. But the fluorescent intensity of the probe did not change with the addition of *E. coli*, even with the addition of zinc ions. These results indicated that the probe can selectively be disassembled by Gram-positive bacteria but not by Gram-negative bacteria. We may conclude that only the hydrophobicity of the bacteria cell walls was not enough to disassemble the aggregates. Gram-positive bacteria and Gram-negative bacteria can be visually distinguished by naked eyes (Figure 3b). The probe with *B. cereus* and *E. coli* showed strong and blue fluorescence (λ_{em} = 450 nm in Figure 1a), respectively, whereas the probe itself displayed green emission (λ_{em} = 500 nm in Figure 1a).

3.3. Wash-Free Fluorescent Imaging of Bacteria. The wash-free imaging of bacteria can simplify the staining protocol and be favorable for bacteria dynamics imaging in situ. Because of the unique enhanced emission responses of **ZTRS-BP** to bacteria sensing, we anticipated that the probe could have excellent Gram-positive bacteria imaging performance without the washing step. To verify this, we carried out bacterial imaging experiments by incubating Gram-positive bacteria *B. cereus* with 5 μM **ZTRS-BP** with or without the addition of Zn^{2+}. And the fluorescent imaging was directly performed without subsequent washing steps. As shown in Figure 4, it is clearly shown that **ZTRS-BP** stained the cell walls of *B. cereus* whether zinc ions were present or not. Also, *B. cereus* can be clearly visualized with great signal-to-noise ratio. To visually present the fluorescent intensity value, we obtained the in situ fluorescent intensity spectra along the red lines in Figure 4b, e to display in Figure 4c, f, respectively. Line 1 in Figure 4c indicated that the fluorescence intensity on the cell wall (~900 au) was 4 times higher than that outside (~200 au), and nearly 2 times higher than that inside the bacteria (~500 au). Meanwhile, it is worth noting that the intensity on the cell walls of the bacteria incubated with zinc ions (~1300−1600 au) were 7 times stronger than that outside (~200 au), and nearly 3 times than that inside the bacteria (~450 au). The results indicated that the wash-free fluorescent images of bacteria incubated with both **ZTRS-BP** and zinc ions had a higher signal-to-noise ratio. Moreover, *B. cereus* were clearly visualized with great signal-to-noise ratio regardless of washing or not washing the bacteria after staining as shown in Figure S3. Above all, the fluorescent imaging results demonstrated that the aggregated probe efficiently illuminated *B. cereus*. This

https://dx.doi.org/10.1021/acsabm.0c01269
ACS Appl. Bio Mater. XXXX, XXX, XXX−XXX

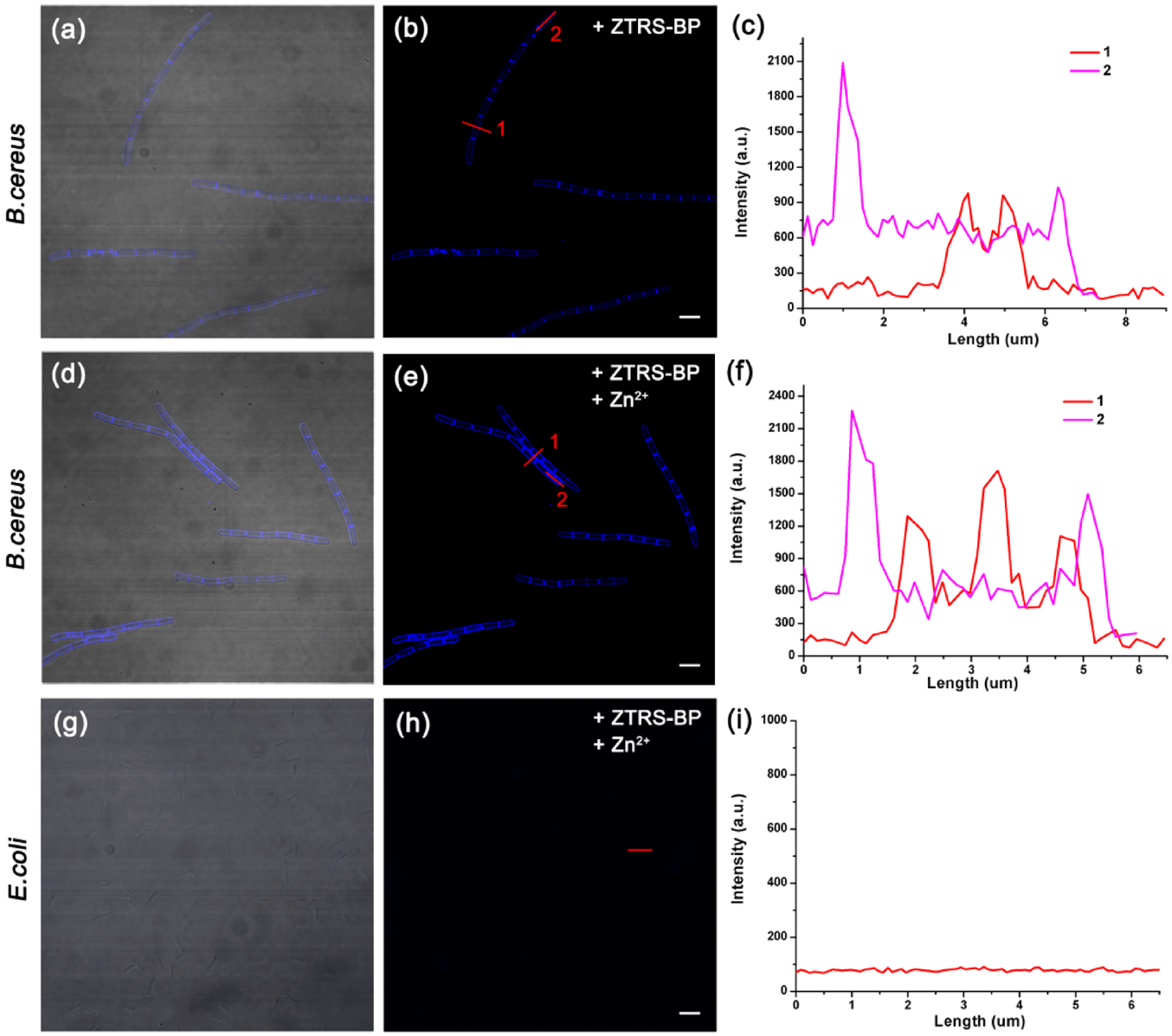

Figure 4. Confocal fluorescent imaging of bacteria loaded with **ZTRS-BP.** (a, b) Fluorescence imaging of *B. cereus* stained with 5 μM **ZTRS-BP** for 10 min in HEPES (10 mM, pH 7.4); (c) fluorescence intensity in situ of the lines in b; (d, e) fluorescence imaging of *B. cereus* stained with 5 μM **ZTRS-BP** and 5 μM Zn^{2+} for 10 min in HEPES; (f) fluorescence intensity in situ of the lines in e; (g, h) fluorescence imaging of *E. coli* stained with 5 μM **ZTRS-BP** and 5 μM Zn^{2+} for 10 min in HEPES; (i) in situ fluorescence intensity of the line in h; a, d, and g are merged imaging of bright-field and fluorescence imaging; Ex: 405 nm; scale bar: 5 μm.

fluorogenic probe based on the aggregation-disaggregation strategy well realized the no-wash imaging of Gram-positive bacteria.

Furthermore, we also observed the division site of *B. cereus* indicated by brighter fluorescence (Figure 4b, e). The fluorescent intensity at division sites (~2000 au, line 2 in Figure 4c, f) were higher than that on the sidewall, existing excellent signal-to-noise ratio (10 times) to the background. Early models of bacterial cell growth held that new peptidoglycan (PG) was made and incorporated at midcell during the time of cell division.[38] In previous reports, fluorescent probes conjugated with the antibiotics vancomycin or ramoplanin were demonstrated to stain the Gram-positive bacteria by targeting PG.[26,39] Because of the similar imaging results, we believed that our probe **ZTRS-BP** also stained the PG layer of the Gram-positive bacteria. After all, **ZTRS-BP-Zn(II)** complex works as an excellent fluorogenic probe to label *B. cereus* cell wall.

3.4. Selective Fluorescence Imaging of Gram-Positive Bacteria. The fluorescent imaging of **ZTRS-BP-Zn(II)** to Gram-negative bacteria *E. coli* was further detected, as shown in Figure 4g−i. The emission with *E. coli* was barely observed, which were consistent with the fluorescence response of the probe in the presence of bacteria in solutions (Figure 3). So, the probe has an excellent staining-specificity toward *B. cereus*. We also imaged other Gram-positive bacteria such as *Staphylococcus aureus* (*S. aureus*) and Gram-negative bacteria such as *Klebsiella pneumoniae* (*K. pneumoniae*) to examine the selectivity of the probe. As shown in Figure S4, *S. aureus* were well labeled by the probe to clearly display the fluorescence on the cell walls. On the contrary, there was no fluorescence detected in the presence of *K. pneumoniae*.

https://dx.doi.org/10.1021/acsabm.0c01269
ACS Appl. Bio Mater. XXXX, XXX, XXX−XXX

To further verify the capability of **ZTRS-BP-Zn(II)** to recognize Gram-positive bacteria over Gram-negative bacteria, we cocultured *B. cereus* and *E. coli* in the same dish and stained with both **ZTRS-BP-Zn(II)** (5 μM) and commercial bacteria cell wall dye **FM4−64** (6 μM) (Figure 5). It was found that *B. cereus* with a rodlike shape were selectively "lit-up" by **ZTRS-BP-Zn(II)**, whereas almost no **ZTRS-BP-Zn(II)** fluorescent signal was observed from *E. coli* (Figure 5a). **FM4−64** can stain both Gram-positive and Gram-negative bacteria (Figure 5b). The merged imaging in Figure 5c showed that, on the *B. cereus* cell wall, there was an alternating fluorescent signals between **ZTRS-BP-Zn(II)** and **FM4−64.** This may be due to the different binding ability of these two dyes to the cell wall.

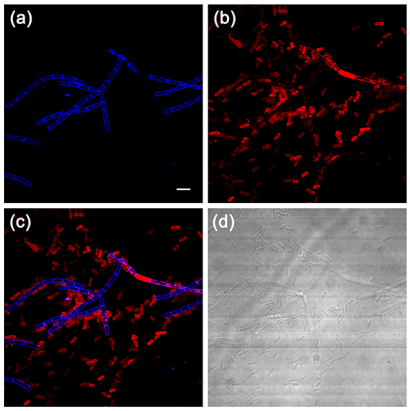

Figure 5. Confocal fluorescence imaging of *B. cereus* and *E. coli* mixture loaded with **ZTRS-BP-Zn(II)** and commercial dye FM4−64. (a) Fluorescent image when excited at 405 nm; (b) fluorescent image when excited at 543 nm; (c) merged image of a and b; (d) bright-field image; scale bar is 5 μm.

And the binding capability of **ZTRS-BP-Zn(II)** may be higher than that of **FM4−64**, because most of the *B. cereus* were brightly stained with **ZTRS-BP-Zn(II)**, but not **FM4−64.** These results demonstrated the excellent performance of **ZTRS-BP-Zn(II)** for accurate identification of Gram-positive bacteria through fluorescent imaging technique. The significant structural difference of outer envelopes between Gram-positive and Gram-negative bacteria may be the reason for the effective identification by **ZTRS-BP-Zn(II)**. As mentioned above, we hypothesized that the probe was bound to the PG of Gram-positive bacteria. However, the outer cell layer of Gram-negative bacteria was composed of the phospholipid bilayer, and PG was on the inner side of the bilayer, which may be the reason why the probe was unable to label Gram-negative bacteria. According to the results above, **ZTRS-BP-Zn(II)** complex was probed to be an excellent dye for wash-free Gram-positive bacteria imaging.

3.5. Fluorescence Imaging of Live/Dead Gram-Positive Bacteria. The detection of bacterial viability is of great significance for determining the survival status of bacteria and monitoring the bactericidal effects of antibiotics.[40] Membrane integrity is an accepted biomarker for viable cells, as cells with compromised membrane are approaching death or already dead.[41] So far, two types of fluorescent dye can be used to determine membrane integrity. One is the dyes permeating into intact cells, such as SYTO 9 and Hoechst 33342. Another is the one that can permeate only compromised cells, such as propidium iodide (PI) and SYTOX Green. The detection of bacterial viability usually uses dual-staining kits such as Live/Dead *Bac*Light Bacterial Viability kit, which contains SYTO 9 and PI fluorescence dyes. The disadvantage of this method is that two dyes must be used at the same time and the dye SYTO 9 is very expensive.

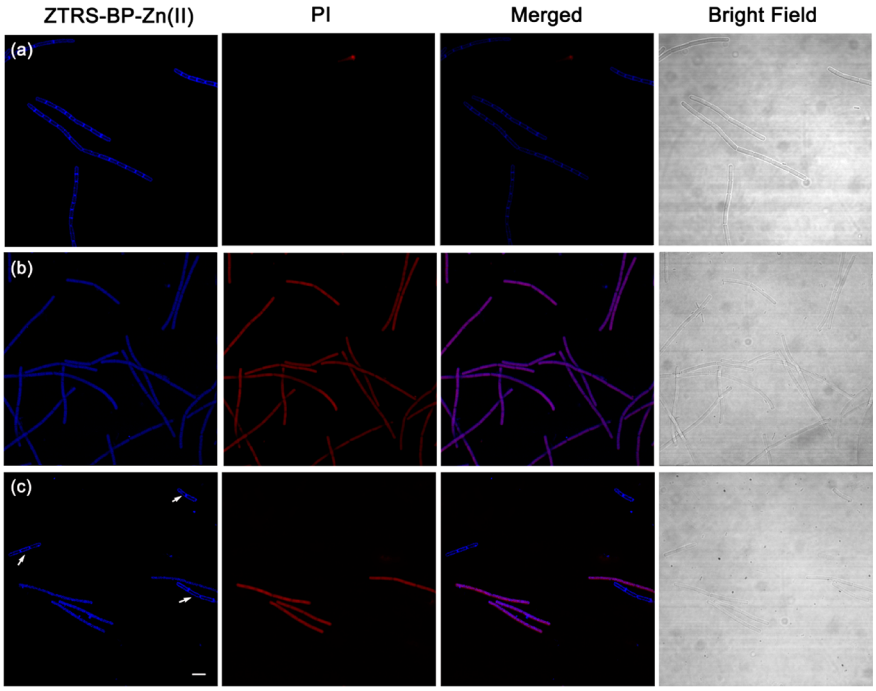

Figure 6. Confocal fluorescence imaging of (a) live, (b) dead, and (c) live/dead mixture of *B. cereus* with **ZTRS-BP-Zn(II)** and commercial dye PI. The first column is the image when excited at 405 nm; the second column is the image when excited at 543 nm; the third column is the merged image; the fourth column is the bright-field image; scale bar is 5 μm.

https://dx.doi.org/10.1021/acsabm.0c01269
ACS Appl. Bio Mater. XXXX, XXX, XXX−XXX

On the basis of the excellent fluorescent imaging property of **ZTRS-BP-Zn(II)** to Gram-positive bacteria, we then further investigated whether **ZTRS-BP-Zn(II)** could show different labeling effects on live and dead Gram-positive bacteria. The live *B. cereus* bacteria and the dead *B. cereus* bacteria obtained by treating with 70% isopropanol were incubated with **ZTRS-BP-Zn(II)**, respectively. We also added the commercial red dye PI, which can only enter the bacteria with compromised cell membranes and bind to DNA. The fluorescent imaging was subsequently obtained without washing steps. As shown in Figure 6a, **ZTRS-BP-Zn(II)** was labeled on the cell wall of *B. cereus*, and there was almost no fluorescence of PI, indicating the survival status of the bacteria. Meanwhile, both of the dyes entered into isopropanol-treated *B. cereus* (Figure 6b). And the dead *B. cereus* can be clearly visualized with great signal-to-noise ratio. Significantly, the merged imaging in Figure 6b indicated that every single bacterium was stained by **ZTRS-BP-Zn (II)** as well as the probe may bind to DNA of dead bacterial. We then mixed the live and dead *B. cereus* in equal amounts, and then the mixed bacteria were incubated with **ZTRS-BP-Zn(II)** and imaged immediately. As shown in Figure 6c, we can clearly see that **ZTRS-BP-Zn(II)** can bind on a certain amount of bacteria cell wall (pointed by white arrows) as well as PI cannot. This *B. cereus* must be live bacteria. Meanwhile, numbers of *B. cereus* were labeled by both **ZTRS-BP-Zn (II)** and PI dyes inside the bacteria, which must be dead ones. These results confirmed that the unique dye, **ZTRS-BP-Zn(II)**, had the ability to differentially image both live and dead bacteria in real time, whereas most other dyes only stained live or dead bacteria.

3.6. Real-Time Tracking of Bacteria Viability. After confirming that the **ZTRS-BP-Zn(II)** molecule had different labeling abilities against live and dead bacteria, we subsequently applied this probe to real-time track bacterial viability by imaging *B. cereus* incubated with antibiotic. vancomycin is a clinically special antibacterial drug. It has a particularly powerful bactericidal effect on Gram-positive bacteria. We added vancomycin to the Gram-positive bacteria *B. cereus*, incubated for 1 h, and then treated the bacteria with **ZTRS-BP-Zn(II)** and imaged it immediately. As shown in Figure 7, most of the bacterial cell walls were intact and clearly marked by the probe, whereas two bacterium were greatly strained inside the bacteria (pointed by white arrows). The reason was that vancomycin compromised *B. cereus* cell wall and the dyes entered into the bacteria. This proves that **ZTRS-BP-Zn(II)** can real-time track antibiotic-interacted Gram-positive bacteria viability. The performance of the probe makes it a powerful tool for real-time tracking bacterial viability for rapid detection of drug sensitivity.

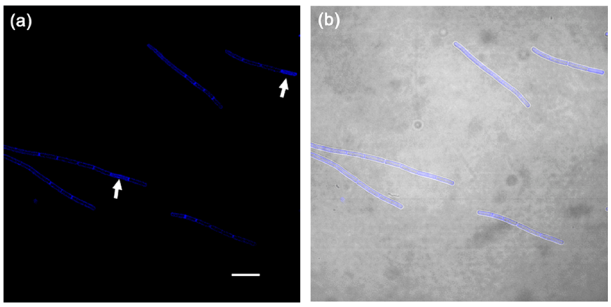

Figure 7. Confocal fluorescent imaging of vancomycin-incubated *B. cereus* with **ZTRS-BP-Zn(II)**. (a) Fluorescence image when excited at 405 nm, the arrows point to the dead bacteria killed by vancomycin; (b) merged imaging of a and bright field; scale bar: 10 μm.

4. CONCLUSION

In summary, we developed a fluorogenic probe **ZTRS-BP** for wash-free fluorescent imaging of Gram-positive bacteria. The probe was constructed by linking a hydrophobic alkyl chains to environment-sensitive probe **ZTRS**. The fluorogenicity was derived from aggregation-caused fluorescence quenching (ACQ) effect of the probe in the aqueous solution. The aggregate can be disassembled by Gram-positive bacteria and emitted fluorescence. The bacterial cell walls were "lit-up" by strong interactions with the dispersed probe. Furthermore, the binding of zinc ions (**ZTRS-BP-Zn(II)**) can enhance the fluorescent signal on the bacterial surface by inhibiting the process of photoinduced electron transfer. Benefiting from its excellent wash-free fluorescent imaging feature for Gram-positive bacteria, **ZTRS-BP-Zn(II)** can either rapidly discriminate Gram-positive bacteria over Gram-negative bacteria or real-time monitor live and dead Gram-positive bacteria through a fluorescence imaging technique. The performance of the probe makes it a powerful tool for real-time tracking bacterial viability for rapid detection of drug sensitivity, which indicates its potential application value in the fields of safety of food and drinking water and environmental and medical microbiology.

■ ASSOCIATED CONTENT

Supporting Information

The Supporting Information is available free of charge at https://pubs.acs.org/doi/10.1021/acsabm.0c01269.

Synthesis detail of the probe and additional figures (PDF)

■ AUTHOR INFORMATION

Corresponding Authors

Lu Miao − *CAS Key Laboratory of Separation Science for Analytical Chemistry, Dalian Institute of Chemical Physics, Chinese Academy of Sciences, Dalian 116023, China*; Email: miaolu@dicp.ac.cn

Xiaolian Li − *State Key Laboratory of Fine Chemicals, Dalian University of Technology, Dalian 116012, China*; Email: xlianlid@163.com

Zhaochao Xu − *State Key Laboratory of Fine Chemicals and Zhang Dayu Schoole of Chemistry, Dalian University of Technology, Dalian 116012, China; CAS Key Laboratory of Separation Science for Analytical Chemistry, Dalian Institute of Chemical Physics, Chinese Academy of Sciences, Dalian 116023, China*; orcid.org/0000-0002-2491-8938; Email: zcxu@dicp.ac.cn

Authors

Weiwei Liu − *State Key Laboratory of Fine Chemicals, Dalian University of Technology, Dalian 116012, China; CAS Key Laboratory of Separation Science for Analytical Chemistry, Dalian Institute of Chemical Physics, Chinese Academy of Sciences, Dalian 116023, China*

Ruihua Li − *The Second Affiliated Hospital of Dalian Medical University, Dalian 116023, China*

Fei Deng − *CAS Key Laboratory of Separation Science for Analytical Chemistry, Dalian Institute of Chemical Physics,*

Chinese Academy of Sciences, Dalian 116023, China; School of Chemistry and Chemical Engineering, Jinggangshan University, Ji'an, Jiangxi 343009, China

Chunyu Yan − *CAS Key Laboratory of Separation Science for Analytical Chemistry, Dalian Institute of Chemical Physics, Chinese Academy of Sciences, Dalian 116023, China; Zhang Dayu Schoole of Chemistry, Dalian University of Technology, Dalian 116012, China*

Xuelian Zhou − *CAS Key Laboratory of Separation Science for Analytical Chemistry, Dalian Institute of Chemical Physics, Chinese Academy of Sciences, Dalian 116023, China; Zhang Dayu Schoole of Chemistry, Dalian University of Technology, Dalian 116012, China*

Complete contact information is available at: https://pubs.acs.org/10.1021/acsabm.0c01269

Author Contributions

†W.L. and R.L. contributed equally to this work. All authors have contributed to the completion of the manuscript. Approval of all the authors has been given for the final manuscript.

Notes

The authors declare no competing financial interest.

■ ACKNOWLEDGMENTS

We are grateful for the financial support from the National Natural Science Foundation of China (22078314, 21878286, 21908216, 21576043), Dalian Institute of Chemical Physics (DICPI201938, DICP I202006), Dalian Talent Support Program (2018RQ16), and Liaoning Provincial Fund (2019JH2/10300016).

■ REFERENCES

(1) *Antibiotic Resistance Threats in the United States, 2013.*Centers for Disease Control and Prevention: Atlanta, 2013.

(2) Thigpen, M. C.; Whitney, C. G.; Messonnier, N. E.; Zell, E. R.; Lynfield, R.; Hadler, J. L.; Harrison, L. H.; Farley, M. M.; Reingold, A.; Bennett, N. M.; Craig, A. S.; Schaffner, W.; Thomas, A.; Lewis, M. M.; Scallan, E.; Schuchat, A. Bacterial meningitis in the United States, 1998−2007. *N. Engl. J. Med.* **2011**, *364*, 2016−2025.

(3) Gaca, J. G.; Sheng, S.; Daneshmand, M. A.; O'Brien, S.; Rankin, J. S.; Brennan, J. M.; Hughes, G. C.; Glower, D. D.; Gammie, J. S.; Smith, P. K. Outcomes for endocarditis surgery in North America: a simplified risk scoring system. *J. Thorac. Cardiovasc. Surg.* **2011**, *141*, 98−106.

(4) *Global Tuberculosis Control: WHO Report 2010*; World Health Organization: Geneva, Switzerland, 2010.

(5) Kollef, M. H.; Bassetti, M.; Francois, B. The intensive care medicine research agenda on multidrug-resistant bacteria, antibiotics, and stewardship. *Intensive Care Med.* **2017**, *43*, 1187−1197.

(6) Levy, S. B; Marshall, B. Antibacterial resistance worldwide: causes, challenges and responses. *Nat. Med.* **2004**, *10*, S122−S129.

(7) *Global Tuberculosis Report 2019*; World Health Organization: Geneva, Switzerland, 2019.

(8) Miao, L.; Liu, W. W.; Qiao, Q. L.; Li, X. L.; Xu, Z. C. Fluorescent antibiotics for real-time tracking of pathogenic bacteria. *J. Pharm. Anal.* **2020**, *10*, 444−451.

(9) Yang, L.; Xiong, H.; Su, Y.; Tian, H.; Liu, X.; Song, X. A red-emitting water-soluble fluorescent probe for biothiol detection with a large Stokes shift. *Chin. Chem. Lett.* **2019**, *30*, 563−565.

(10) Wen, Y.; Huo, F. J.; Yin, C. X. Organelle targetable fluorescent probes for hydrogen peroxide. *Chin. Chem. Lett.* **2019**, *30*, 1834−1842.

(11) Qin, H.; Li, L.; Li, K.; Xiaoqi, Y. Novel strategy of constructing fluorescent probe for MAO-B *via* cascade reaction and its application in imaging MAO-B in human astrocyte. *Chin. Chem. Lett.* **2019**, *30*, 71−74.

(12) Kang, Y. F.; Niu, L. Y.; Yang, Q. Z. Fluorescent probes for detection of biothiols based on "aromatic nucleophilic substitution-rearrangement" mechanism. *Chin. Chem. Lett.* **2019**, *30*, 1791−1798.

(13) Hu, G. D.; Jia, H. Y.; Zhao, L. N.; Cho, D. H.; Fang, J. G. Small molecule fluorescent probes of protein vicinal dithiols. *Chin. Chem. Lett.* **2019**, *30*, 1704−1716.

(14) Keer, J. T.; Birch, L. Molecular methods for the assessment of bacterial viability. *J. Microbiol. Methods* **2003**, *53*, 175−183.

(15) Stiefel, P.; Schmidt-Emrich, S.; Maniura-Weber, K.; Ren, Q. Critical aspects of using bacterial cell viability assays with the fluorophores SYTO9 and propidium iodide. *BMC Microbiol.* **2015**, *15*, 36−44.

(16) Zeng, D. X.; Chen, Z.; Jiang, Y.; Xue, F.; Li, B. G. Advances and challengesin viability detection of foodborne pathogens. *Front Microbiol.* **2016**, *7*, 1−12.

(17) Phetsang, W.; Pelingon, R.; Butler, M. S.; Kc, S.; Pitt, M. E.; Kaeslin, G.; Cooper, M. A.; Blaskovich, M. A. T. Fluorescent trimethoprim conjugate probes to assess drug accumulation in wild type and mutant Escherichia coli. *ACS Infect. Dis.* **2016**, *2*, 688−701.

(18) Tang, J. L.; Chu, B. B.; Wang, J. H.; Song, B.; Su, Y. Y.; Wang, H. Y.; He, Y. Multifunctional nanoagents for ultrasensitive imaging and photoactive killing of Gram-negative and Gram-positive bacteria. *Nat. Commun.* **2019**, *10*, 4057.

(19) Woo, P.C.Y.; Lau, S.K.P.; Teng, J.L.L.; Tse, H; Yuen, K.-Y. Then and now: use of 16S rDNA gene sequencing for bacterial identifification and discovery of novel bacteria in clinical microbiology laboratories. *Clin. Microbiol. Infect.* **2008**, *14*, 908−934.

(20) van Oosten, M.; Schafer, T.; Gazendam, J. A. C.; Ohlsen, K.; Tsompanidou, E.; de Goffau, M. C.; Harmsen, H. J. M.; Crane, L. M. A.; Lim, E.; Francis, K. P.; et al. Real-time in vivo imaging of invasive- and biomaterial-associated bacterial infections using fluorescently labelled vancomycin. *Nat. Commun.* **2013**, *4*, 2584−2591.

(21) Petchiappan, A.; Chatterji, D. Antibiotic resistance: current perspectives. *ACS Omega* **2017**, *2*, 7400−7409.

(22) Chen, W. W.; Li, Q. Z.; Zheng, W. S.; Hu, F.; Zhang, G. X.; Wang, Z.; Zhang, D. Q.; Jiang, X. Y. Identification of bacteria in water by a fluorescent array. *Angew. Chem., Int. Ed.* **2014**, *53*, 13734−13739.

(23) He, P.; Lv, F. T.; Liu, L. B.; Wang, S. Cationic conjugated polymers for detection and inactivation of pathogens. *Sci. China: Chem.* **2017**, *60*, 1567−1574.

(24) Kuru, E.; Hughes, H. V.; Brown, P. J.; Hall, E.; Tekkam, S.; Cava, F.; de Pedro, M. A.; Brun, Y. V.; Van Nieuwenhze, M. S. In situ probing of newly synthesized peptidoglycan in live bacteria with fluorescent D-amino acids. *Angew. Chem., Int. Ed.* **2012**, *51*, 12519−12523.

(25) Morris, M. A.; Malek, M.; Hashemian, M. H.; Nguyen, B. T.; Manuse, S.; Lewis, K.; Nowick, J. S. A fluorescent teixobactin analogue. *ACS Chem. Biol.* **2020**, *15*, 1222−1231.

(26) Tiyanont, K.; Doan, T.; Lazarus, M. B.; Fang, X.; Rudner, D. Z.; Walker, S. Imaging peptidoglycan biosynthesis in Bacillus subtilis with fluorescent antibiotics. *Proc. Natl. Acad. Sci. U. S. A.* **2006**, *103*, 11033−11038.

(27) Wang, H. Y.; Hua, X. W.; Jia, H. R.; Li, C. C.; Lin, F. M.; Chen, Z.; Wu, F. G. Universal cell surface imaging for mammalian, fungal, and bacterial cells. *ACS Biomater. Sci. Eng.* **2016**, *2*, 987−997.

(28) Huang, Y.; Pappas, H. C.; Zhang, L.; Wang, S. S.; Cai, R.; Tan, W. H.; Wang, S.; Whitten, D. G.; Schanze, K. S. Selective imaging and inactivation of bacteria over mammalian cells by imidazolium-substituted polythiophene. *Chem. Mater.* **2017**, *29*, 6389−6395.

(29) Kwon, H. Y.; Liu, X.; Choi, E. G.; Lee, J. Y.; Choi, S. Y.; Kim, J. Y.; Wang, L.; Park, S. J.; Kim, B.; Lee, Y. A.; Kim, J. J.; Kang, N. Y.; Chang, Y. T. Development of a universal fluorescent probe for Gram-positive bacteria. *Angew. Chem., Int. Ed.* **2019**, *58*, 8426−8431.

(30) Gao, M.; Hu, Q. L.; Feng, G. X.; Tomczak, N.; Liu, R. R.; Xing, B. G.; Tang, B. Z.; Liu, B. A multifunctional probe with aggregation-induced emission characteristics for selective fluorescence imaging

and photodynamic killing of bacteria over mammalian cells. *Adv. Healthcare Mater.* **2015**, *4*, 659−663.

(31) Wang, W.; Lin, L. Y.; Du, Y. H.; Song, Y. L.; Peng, X. M.; Chen, X.; Yang, C. Y. J. Assessing the viability of transplanted gut microbiota by sequential tagging with D-amino acid-based metabolic probes. *Nat. Commun.* **2019**, *10*, 1317−1323.

(32) Geva-Zatorsky, N.; Alvarez, D.; Hudak, J. E; Reading, N. C; Erturk-Hasdemir, D.; Dasgupta, S.; von Andrian, U. H; Kasper, D. L In vivo imaging and tracking of host-microbiota interactions via metabolic labeling of gut anaerobic bacteria. *Nat. Med.* **2015**, *21*, 1091−1100.

(33) Shieh, P.; Siegrist, M. S.; Cullen, A. J.; Bertozzi, C. R. Imaging bacterial peptidoglycan with near-infrared fluorogenic azide probes. *Proc. Natl. Acad. Sci. U. S. A.* **2014**, *111*, 5456−5461.

(34) Long, S. S.; Qiao, Q. L.; Miao, L.; Xu, Z. C. A self-assembly/disassembly two-photo ratiometric fluorogenic probe for bacteria imaging. *Chin. Chem. Lett.* **2019**, *30*, 573−576.

(35) Xu, Z. C.; Baek, K. H.; Kim, H. N.; Cui, J. N.; Qian, X. H.; Spring, D. R.; Shin, I.; Yoon, J. Y. Zn^{2+}-triggered amide tautomerization produces a highly Zn^{2+}-selective, cell-permeable, and ratiometric fluorescent sensor. *J. Am. Chem. Soc.* **2010**, *132*, 601−610.

(36) Deng, F.; Long, S. S.; Qiao, Q. L.; Xu, Z. C. The environmental-sensitivity of a fluorescent ZTRS-Cd(ii) complex was applied to discriminate different types of surfactants and determine their CMC values. *Chem. Commun.* **2018**, *54*, 6157−6160.

(37) Deng, F.; Liu, L. M.; Qiao, Q. L.; Huang, C. F.; Miao, L.; Xu, Z. C. A general strategy to develop cell membrane fluorescent probes with location- and target-specific fluorogenicities: a case of a Zn2+ probe with cellular selectivity. *Chem. Commun.* **2019**, *55*, 15045−15048.

(38) Bramhill, D. Bacteria cell division. *Annu. Rev. Cell Dev. Biol.* **1997**, *13*, 395−424.

(39) Daniel, R. A.; Errington, J. Control of cell morphogenesis in bacteria: two distinct ways to make a rod-shaped cell. *Cell* **2003**, *113*, 767−776.

(40) Kumar, S. S.; Ghosh, A. R. Assessment of bacterial viability: a comprehensive review on recent advances and challenges. *Microbiology* **2019**, *165*, 593−610.

(41) Emerson, J. B.; Adams, R. I.; Roman, C. M. B.; Brooks, B.; Coil, D. A.; Dahlhausen, K.; Ganz, H. H.; Hartmann, E. M.; Hsu, T.; Justice, N. B.; et al. Schrödinger's microbes: tools for distinguishing the living from the dead in microbial ecosystems. *Microbiome* **2017**, *5*, 86.

https://dx.doi.org/10.1021/acsabm.0c01269
ACS Appl. Bio Mater. XXXX, XXX, XXX−XXX